*Laser and Particle Beams* (1996), *vol.* 14, *no.* 3, *pp.* 369–384
Printed in the United States of America



# General features of highly charged ion generation in laser-produced plasmas

**By I.V. ROUDSKOY**
Institute of Theoretical and Experimental Physics, 117259 Moscow, Russia

(Received 29 March 1996; accepted 17 April 1996)

The simple physical model of highly charged ion generation in plasma produced by laser irradiation with long pulse duration (>1 ns) and moderate intensities ($<10^{15}/\lambda^2$ W/cm$^2$ $\mu$m$^2$) is presented. In the frame of a single theory, most of the experimental results on plasma diagnostics are described in total. It is shown that plasma temperatures, ion charge states, and ion velocities as well as angular distributions of highly charged ions can be explained with good accuracy by collisional absorption of laser energy, hydrodynamic acceleration of forming plasma, and three-body recombination through highly exited levels during plasma expansion into vacuum. The general scalings for plasma parameters are derived on the basis of the model proposed.

## 1. Introduction

The interaction of laser radiation with solid targets is a very complicated process that includes a great number of diverse mechanisms, some of them still under discussion even today. Nevertheless, in each specific case a restricted quantity of main mechanisms can be picked out from this variety, preserving general features of the phenomenon observed. The concrete choice depends on the plasma parameters to be obtained, the demanded result accuracy, and a laser installation that has been used for plasma production.

The paper presents a simple physical model of highly charged ion generation in a plasma produced by a laser radiation with a moderate intensity (from $10^{10}$ up to $10^{14}$–$10^{15}$ W/cm$^2$ for Nd glass laser and from $10^9$ to $10^{12}$–$10^{13}$ W/cm$^2$ for $CO_2$ laser) and a long pulse duration (above 1 ns) acting upon a solid flat target. A choice of this range is conditioned by parameters of lasers that are used now in laser ion sources for heavy ion production (Barabash *et al.* 1989).

On the basis of this model the general dependences of highly charged ion generation were derived and a numerical code was worked out. This code enables us to calculate an ion charge state distribution in plasma at different distances from a target (up to a few meters) as well as other plasma parameters such as electron and ion temperatures and densities, plasma velocity, and some others. The numerical results are shown to be in a good agreement with most of the experimental data in a wide range of laser radiation parameters.

## 2. Heating stage

From the point of view of laser ion source development, the most important plasma parameters that we should explain and calculate are as follows: ion charge state distribution, ion energy distribution, and ion currents (or the number of ions of each charge state produced during the interaction).

All of these are interdependent, and, when working out a physical model of ion generation in laser–target interactions, it is necessary to explain all of the experimental data in

 0263-0346/96 $11.00 + .10

total. Therefore we need to determine the prevalent mechanisms of energy absorption and plasma acceleration as well as ionization and recombination processes on a stage of plasma heating and subsequent expansion into vacuum (since there is usually a rather long drift space between a target and an extraction or analyzing system) under typical experimental conditions.

The following four main parameters of laser radiation should be taken into account in the analysis of laser–target interaction—a pulse duration $\tau_l$, a radiation wavelength $\lambda$, a laser power $P_l$ (or a flux density $I_l$), and a focus spot size $d$.

A regime of laser–target interaction is determined mainly by a laser pulse duration. There are two characteristic time values in the process under consideration: $t_s$—the life-time of skin layer, and $t_d$—the hydrodynamic lift-time of a plasma cloud with a focal spot size. These values depend on the laser flux density, the mass of plasma ions, and so on, but the typical ones are $t_s \approx 1$ ps, $t_d \approx 1$ ns. So there are three clearly distinguishable regimes of laser–target interaction that, in principle, are different:

- Very short pulses, $\tau_l < t_s$, where the absorption of laser energy takes place in a thin skin layer on the surface of a solid target.
- Middle pulse durations, $t_s < \tau_l < t_d$. Here the laser energy is absorbed in a more rare plasma with the density not greater than the critical value $n_{cr}$ for a given laser wavelength on a density profile formed during expansion. The interaction process is nonstationary, and plasma parameters depend on a laser pulse duration.
- Long pulses, $\tau_l > t_d$. In this case, a quasi-stationary process of interaction of an incident laser beam with a steady expanding plasma is realized. It is this case which proceeds in most of the laser facilities for highly charged ion production and will be considered in this paper.

The radiation wavelength $\lambda$ determines a density of hot plasma ($n_{cr} = 10^{19}$ cm$^{-3}$ for $\lambda = 10.6$ $\mu$m and $n_{cr} = 10^{21}$ cm$^{-3}$ for $\lambda = 1.06$ $\mu$m). In the first place, it influences the mechanisms of laser energy absorption and the subsequent transmission of the energy from the absorption area into inner and outer layers. Besides that, the difference in plasma densities calls forth the difference in ionization and recombination rates during laser-pulse interactions with plasma as well as acting upon recombination rates during the following plasma expansion into vacuum, which will be shown later.

If not too high laser flux intensities [$I_l\lambda^2$ below $10^{15}$ W/cm$^2$ $\mu$m$^2$ (Basov *et al.* 1983)] are used for plasma production, the prevalent mechanism of laser energy absorption in these conditions is the classical inverse Bremsstrahlung absorption (in other words—collisional absorption). The typical plasma temperature in this case can vary from 100 eV to a few keV for short wavelengths ($\lambda = 1.06$ $\mu$m) and to 300–400 eV for a long ($\lambda = 10.6$ $\mu$m) wavelength radiation. It is simple to make sure that under typical spot sizes, $d = 50$–$500$ $\mu$m, the behavior of a plasma with these parameters can be described in the frame of hydrodynamics [see, e.g., Basov *et al.* (1986)].

This regime of laser–target interaction was examined in detail in a great number of works [see, e.g., Afanasiev *et al.* (1976) and Demchenko *et al.* (1988)], but the comprehensive comparative analysis at first was done in Latyshev and Roudskoy (1986, 1987). The predominate mechanism of energy transmission from the absorption area for flux intensities $I_l/\lambda > 10^{10}$ W/cm$^2$/$\mu$m was shown to be an electron heat conduction. The expression for the thermal flux strongly depends on a radiation wavelength. It is described by a common equation with Spitzer's thermal conductivity $q_e = \kappa \nabla T_e$ for short wavelength radiations. In the case of a long wavelength, the thermal flux is restricted by the value $q_{\max} = f\sqrt{2/\pi} n_e T_e (T_e/m_e)^{1/2}$. Nevertheless, plasma temperature on a heating stage proved to be practically independent on radiation wavelength:

$$T_e[\text{eV}] \simeq \begin{cases} 100 \cdot (\bar{Z} P_{l[\text{GW}]}/d_{[\text{mm}]})^{2/7} \sim (\bar{Z} I_l d)^{2/7}, & \lambda = 1.06\ \mu\text{m} \\ 100 \cdot (\bar{Z} P_{l[\text{GW}]}/d_{[\text{mm}]})^{1/3} \sim (\bar{Z} I_l d)^{1/3}, & \lambda = 10.6\ \mu\text{m}. \end{cases} \quad (1)$$

It happens because the absorbed fraction of incident laser energy is smaller if a long wave radiation is used. In the last case, a large number of hot electrons can occur. It is usually attributed to other mechanisms of laser energy absorption such as a resonant absorption, for example (Gus'kov *et al.* 1983). Because these electrons do not take a marked part in ionization processes (due to a very little cross section $\sigma \sim 1/v^3$ compared with thermal electrons) and leave the absorption area, according to estimation, without appreciable energy deposition, this effect can be neglected in the problem under consideration. Therefore, the term $T_e$ in this paper will stand for a temperature of thermal electrons in eV.

In the work by Latyshev and Roudskoy (1986) the factor $f = 1$ was used in the expression for restricted thermal flux. Numerical simulations carried out in the current paper showed that plasma temperature does not change if we suppose $f$ to be in the interval 0.1–1. It results from a steeping plasma profile with a decrease in $f$ and an appropriate decrease in the fraction of absorbed laser energy. Thus the meaning of $f$ mainly affects a mass of vapored matter. The same values of the factor $f$ were obtained in a separate set of experimental measurements (Volenko *et al.* 1983; Anuchin *et al.* 1989).

One more important relationship should be noted—an increase in a spot size $d$ leads to an increase in plasma temperature at the same flux intensity $I_l$.

Numerous experimental results of plasma temperature measurements in the range from 50 eV to a few keV collected and adduced in the work by Latyshev and Roudskoy (1986) conclusively confirm the scaling low obtained. Figure 1, borrowed from that paper without source references, presents the experimental data by different experimental groups and scaling lows as a function of $\bar{Z} P_l/d$.

The term $\bar{Z}$ in equation (1) is an average ion charge state in a plasma during its heating. The average ion charge states in plasmas produced by a short wavelength radiation were shown (Latyshev & Roudskoy 1987) to be higher compared with the case of long wavelength radiations at the same plasma temperature. This is caused by the suppression of the dielectronic recombination (possessing the highest rate) in a more dense plasma. Therefore, in a plasma with $n_{cr} = 10^{21}\ \text{cm}^{-3}$, the ion charge state distribution is close to coronal equilibrium; whereas in a more rare plasma, $n_{cr} < 10^{20}\ \text{cm}^{-3}$, the ion charge states are determined by equilibrium between impact ionization and dielectronic recombination. In most of the cases under consideration, there is enough time for the two equilibriums to be established.

The average charge state $\bar{Z}$ can be estimated by using analytical expressions for the ionization and recombination rates, replacing $Z$ with $\bar{Z}$. So using the semiempirical Seaton's equation for the ionization rate (Veinstein *et al.* 1979):

$$\mathcal{K}_z^i \simeq 4.3 \cdot 10^{-8} m (Ry/I_z)^{3/2} (I_z/T_e)^{-1/2} e^{-I_z/T_e} \quad \text{cm}^3/\text{s}, \quad (2)$$

the expression from McWirter (1965) for radiative recombination:

$$\mathcal{R}_z^r \simeq 2 \cdot 10^{-13} Z^2/T_e^{1/2} \quad \text{cm}^3/\text{s}, \quad (3)$$

and the simplified Burdgess' equation from Latyshev and Roudskoy (1987) for the rate of dielectronic recombination:

$$\mathcal{R}_z^d \simeq 6 \cdot 10^{-6} m (Z/T_e)^{3/2} I_z^{1/2} e^{-I_z/T_e} \quad \text{cm}^3/\text{s}, \quad (4)$$

leads to the following equation set for the estimation of laser-produced plasma parameters on a heating stage:

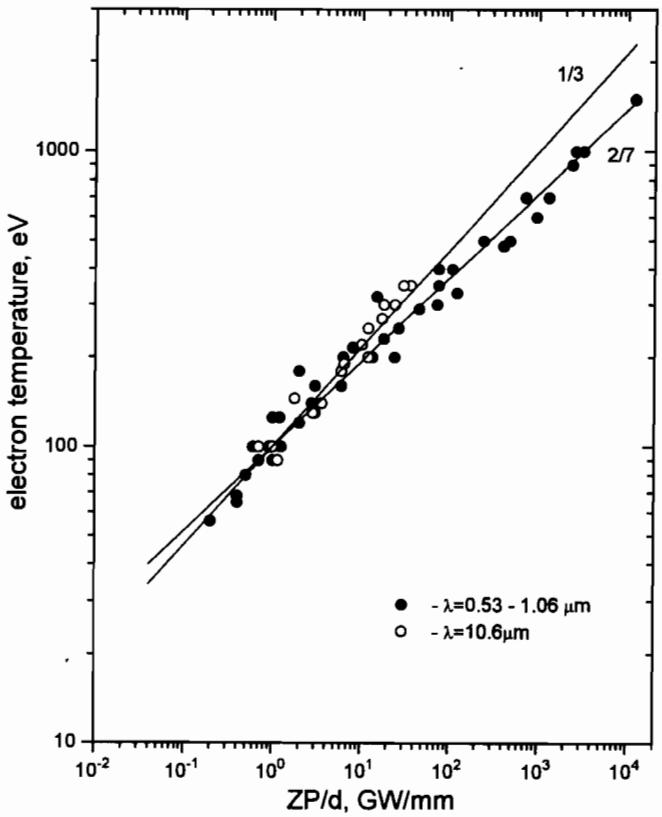


FIGURE 1. Experimental results of plasma temperature measurements and scaling equation (1)].

$$\begin{cases} T_e \simeq 100 \cdot (\bar{Z}P_l/d)^{2/7} \\ e^{I_{\bar{z}}/T_e} \simeq 10^7 T_e m/(I_{\bar{z}}\bar{Z})^2 \end{cases} \tag{5}$$

for short wavelengths and

$$\begin{cases} T_e \simeq 100 \cdot (\bar{Z}P_l/d)^{1/3} \\ I_{\bar{z}}/T_e \simeq 56/(I_{\bar{z}}^{1/4}\bar{Z}^{3/4}) \end{cases} \tag{6}$$

for long wavelengths. Here and in the rest of this paper, $n_e$ is the electron density in $\mathrm{cm}^{-3}$, $Ry \simeq 13.6$ eV, $I_z$ is the ionization potential in eV, and $m$ is the number of equivalent electrons of $(Z-1)$-stripped ions. The typical value of $I_z/T_e$ in this region of plasma parameters is equal to 1.5–2 for $\lambda = 10.6$ $\mu$m and 3–5 for $\lambda = 1.06$ $\mu$m.

Being accelerated hydrodynamically, ions acquire kinetic energy that is much greater than the plasma temperature on a heating stage. Really, even in an adiabatic case (Zeldovich & Raizer 1966) the maximum ion velocity reaches the value $2/(\gamma - 1)v_s$, where, as usual, $\gamma = c_p/c_v$ (equals to 5/3 for plasma) and $v_s$ is a sound velocity:

$$v_s \simeq \left(\frac{5}{3}(Z+1)T_e/m_i\right)^{1/2}.$$

Thus the kinetic ion energy can reach:

$$E_{\mathrm{kin}}^{\max} \simeq 15/2(Z+1)T_e \qquad \text{eV}. \tag{7}$$

The analogous consideration for isothermal expansion brings about an increase in the ion energy by the factor of $\ln(n_{in}/n_{fin}) \approx \ln(\tau_l v_s/d)^3$ compared with the former value (7). Here $n_{in}$ and $n_{fin}$ are the initial and final plasma densities of the isothermal process, respectively.

The numerical simulations carried out showed that the acceleration of plasma took place for the most part during the plasma heating by incident radiation. At that moment the expansion of the plasma cloud courses at intermediate conditions. Thus, a precise value of ion energy can be obtained only by numerical calculation. However, this value considerably exceeds the plasma temperature.

## 3. Plasma expansion into vacuum

The ion charge state distribution does not remain the same after the end of the laser pulse. The experimental measurements (Golubev *et al.* 1984; Tallents 1980) show the decrease in ion charge states as well as the intensive three-body recombination through high exited levels (Afrosimov *et al.* 1984) during plasma expansion at a large range of distances from the target. Because of heavy dependence of the rate of this recombination process (Gurevich & Pitaevsky 1964) on plasma temperature,

$$\mathcal{R}_z^t \simeq 10^{-26} Z^3 n_e / T_e^{9/2} \qquad \text{cm}^3/\text{s}, \tag{8}$$

the energy balance of processes in an expanding plasma becomes important.

It is easy to be convinced that the specific quantity of energy loss due to the work done by the plasma pressure in the adiabatic expansion

$$Q_{\text{hyd}} = \frac{P}{V}\frac{dV}{dt} \sim \frac{n_e T_e}{t} \tag{9}$$

diminishes with time as $t^{-6}$, whereas the fraction of energy returning into the plasma during the three-body recombination,

$$Q_{\text{rec}} = n_i n_e \mathcal{R}_z^t E^* \sim n_e^2 n_i E^* / T^{9/2} \sim E^*, \tag{10}$$

drops as $E^*$—the quantity of energy that is released in an individual act of the recombination—and $Q_{\text{rec}}$ sooner or later becomes comparable with $Q_{\text{hyd}}$, causing extreme disturbances to the initial adiabatic expansion.

This question was examined in detail in Latyshev and Roudskoy (1985), where it was shown that the well-known expression for $E^*$ proposed in Zeldovich and Raizer (1966) and applied by some authors in their calculations (see, e.g., Goforth & Hammerling 1976; Payne *et al.* 1978) gives too high a value for this energy. A new equation for $E^*$ was derived there:

$$E^* \simeq 4.4 \cdot 10^{-10} (n_e/Z)^{2/3}/T_e \qquad \text{eV}, \tag{11}$$

which resulted in a good agreement of the experimental and numerical data.

A qualitative analysis of the behavior of plasma temperature and average ion charge state in an expanding plasma can be done in the following way. Let us consider a Lagrangian liquid shell with the volume $V$. The balance of the electron number in the shell is described by the equation:

$$\frac{dN_e}{dt} = -N_i n_e \mathcal{R}_z^t.$$

Here $N_i$ and $N_e$ are the number of ions and electrons, respectively. Going over from electron density $n_e$ into average ion charge state $Z$, one can write:

$$\frac{dZ}{dt} = -\Re_z^t n_e \simeq 10^{-26} n_i^2 Z^5 / T_e^{9/2}. \tag{12}$$

Using this expression and supposing that $V \sim t^3$, the energy balance for the electron component

$$\frac{3}{2} N_e \frac{dT_e}{dt} = -n_e T_e \frac{dV}{dt} + N_i n_e \Re_z^t E^*$$

can be transformed into

$$\frac{dT_e}{dt} = -2\frac{T_e}{t} + \frac{2}{3}\left(-\frac{dZ}{dt}\right)\frac{E^*}{Z}. \tag{13}$$

(The electron–ion energy exchange was neglected here.) Making the substitution of variables:

$$x = -\frac{d\ln Z}{d\ln t}; \qquad y = \frac{2}{3} x \frac{E^*}{T_e}$$

and differentiating with respect to $\ln x$, the nonlinear equation set (12), (13) can be written as follows:

$$\begin{cases} \dfrac{d\ln x}{d\ln t} = -5 + 4\dfrac{d\ln Z}{d\ln t} - \dfrac{9}{2}\dfrac{d\ln T_e}{d\ln t} \\ \dfrac{d\ln y}{d\ln t} = -7 + 4\dfrac{d\ln Z}{d\ln t} - \dfrac{13}{2}\dfrac{d\ln T_e}{d\ln t}. \end{cases} \tag{14}$$

Eliminating $t$ between the equations, we obtain:

$$\frac{dy}{dx} = \frac{y}{x}\frac{12 - 8x - 13y}{8 - 8x - 9y}. \tag{15}$$

The equation has four singularities:

(0,0) — an unstable node,
(0,12/13) — a stable node,
(1,0) — a saddle with separatrixes $y = 0$ and $y = -4/3x$,
$(-1/8,1)$ — a saddle with separatrixes $y = -0.6x$ and $y = -10x$.

From this one can conclude that under any initial conditions the integral curves converge to the node (0,12/13). Since equation (13) is equivalent to

$$\frac{d\ln T}{d\ln t} = -(2 - y),$$

it corresponds to the following asymptotic behavior of plasma temperature and ion charge state:

$$\begin{cases} T_e \overset{t\to\infty}{\to} r^{-14/13} \\ Z \overset{t\to\infty}{\to} \text{const}, \end{cases} \tag{16}$$

where $r \sim t_{-1}$ is a distance from the target. In other words, the plasma temperature drops with the increase in distance from a target nonadiabatically as $r^{-14/13}$ and the so-called freezing of the ion charge state is put into effect under any initial conditions. Nevertheless, it should be kept in mind that the ion charge states can undergo considerable changes before freezing.

The important consequence of adiabatic expansion ($T_e \sim r^{-2}$) into $T_e \sim r^{-14/13}$ is an existence of a maximum of the function $|dZ/dt| = n_e \Re_z^t$ with respect to $r$ at a point $r_m$. The initial sharp rise of recombination losses $\sim r^3$ changes into a rather slow drop as $r^{-15/13}$. It leads to the fact that the main contribution to the reduction in the average ion charge state

$$\Delta Z(r) = -\int_{r_{in}}^{r} \frac{n_e \Re_z^t}{v}\, dr$$

makes a region near and behind the maximum $r_m$. The value of recombination loss at the maximum and its position can be calculated approximately by equating $Q_{\text{hyd}}$ and $Q_{\text{rec}}$. Supposing a linear distribution of ion velocity in spherical expanding plasma $v(r) = r \cdot v_f / r_f$, where $v_f$ and $r_f$ are front velocity and plasma radius, respectively, one can derive:

$$Q_{\text{hyd}} \simeq 3 n_e T_e v_f / r_f \qquad \text{eV/cm}^3\text{/s}.$$

An expression for $Q_{\text{rec}}$ can be obtained from equation (10) by substituting $\Re_z^t$ and $E^*$ by their values in equations (8) and (11):

$$Q_{\text{rec}} \simeq 4.5 \cdot 10^{-36} \frac{n_e^2 n_i^{5/3}}{T_e^{13/2}} Z^3 \qquad \text{eV/cm}^3\text{/s}.$$

Assuming $n_e \simeq n_{cr}(d/r)^3$ and $T_e \simeq T_{in}(r_{in}/r_f)^2$, where $d$ is a focal spot size, and $T_{in}$ and $r_{in} \simeq v_f \tau_l$ are initial temperature and initial size of a plasma cloud at the end of heating stage, respectively, we are lead to the following equation for $r_m$:

$$T_{in}^{13/2} (v_f \tau_l)^{13} v_f \simeq 1.5 \cdot 10^{-36} n_c^{8/3} Z^{4/3} d^8 r_f^{14} / r_m^8. \tag{17}$$

What is of great interest is not the numerical value of $r_m$ itself, because of a large number of assumptions made during the derivation, but a scaling low for it,

$$r_m \sim \frac{T_e^{13/12} v^{14/6} \tau_l^{13/6}}{n_{cr}^{8/18} d^{8/6}}, \tag{18}$$

and for the maximum value of the function $|dZ/dt|$:

$$\left| \frac{dZ}{dt} \right|_{r=r_m} = n_e \Re_z^t |_{r=r_m} \sim \frac{n_{cr}^2 d^6 r_m^3}{T_{in}^{9/2} r_{in}^9} \sim \frac{n_{cr}^{2/3} d^2}{T_{in}^{5/4} v^2 \tau_l^{5/2}}, \tag{19}$$

which can be obtained from equation (17) using a linear dependence of $v(r)$.

First, these scaling lows explain experimental results of ion spectra measurements (see, e.g., Barabash *et al.* 1984; Tallents 1980)—more energetic ions have higher charge states. Really, from equation (18) one can see the faster ions begin to recombine at greater distances from the target than the slowly moving ions, and their charge state losses [equation (19)] are smaller. It also explains the experimental results with more intense laser pulses (Hora *et al.* 1992) when this dependence disappears—the increase in plasma temperature $T_{in}$ calls forth a shift of the region of high rate recombination at a larger range of distances from the target that can eliminate the ion charge state losses during the plasma expansion (at least for the fastest ion group).

Second, it reveals some ways to improve laser ion source performances. An increase in radiation wavelength as well as an increase in a pulse duration $\tau_l$ and a sharpening of focal spot size $d$, under other equivalent conditions, promote the increase in the highly charged ion yield from a laser ion source.

## 4. Numerical simulation

To calculate exact values of plasma parameters and an ion charge state distribution at different distances from a target, a numerical code was worked out. The following set of Lagrangian equations was solved using a fully conservative differential scheme:

$$\frac{\partial n_1}{\partial t} = -\frac{n_1}{V}\frac{\partial V}{\partial t} \tag{20}$$

$$\rho \frac{\partial u_x}{\partial t} = -\frac{\partial}{\partial x}(p_e + p_i) \tag{21}$$

$$\rho \frac{\partial u_r}{\partial t} = -\frac{2}{r}(p_e + p_i) \tag{22}$$

$$\frac{3}{2}\frac{\partial T_e}{\partial t} + p_e \frac{\partial}{\partial x}\left(\frac{1}{n_e}\right) = \frac{1}{n_e}\left(Q_{las} - Q_{ei} - Q_{ri} - \frac{\partial q_e}{\partial x}\right) \tag{23}$$

$$\frac{3}{2}\frac{\partial T_i}{\partial t} + p_i \frac{\partial}{\partial x}\left(\frac{1}{n_i}\right) = \left(\frac{1}{n_i}\right) Q_{ei} \tag{24}$$

$$\frac{dN_z}{dt} = N_{z-1}\mathcal{K}_{z-1} - N_z\mathcal{R}_z - N_z\mathcal{K}_z + N_{z+1}\mathcal{R}_{z+1}, \qquad Z = 0 \ldots Z_{\max}. \tag{25}$$

It is a two-temperature 1D hydrodynamic code that takes into account lateral expansion. Here $T_i$, $n_i$ are ion temperature and concentration; $p_e$, $p_i$ are electron and ion pressure; $\rho$ is plasma mass density in g/cm$^3$; $u_x$, $u_r$ are normal and radial plasma velocity components ($X$-axis is perpendicular to the target surface); $N_z$ is the number of ions in a $Z$ charge state in a specific volume $v = 1/n_i$; and $\mathcal{K}_z$, $\mathcal{R}_z$ are the total ionization and recombination rates of $Z$ charged ions. The radiative [equation (3)], dielectronic [equation (4)], and three-body recombination [equation (8)] as well as the electron impact ionization [equation (2)] were taken into account.

The electron–ion temperature relaxation is described by the term $Q_{ei}$:

$$Q_{ei} = \frac{3m_e}{m_i} n_e \nu_{ei}(T_e - T_i),$$

where $m_e$, $m_i$ are electron and ion masses; and $\nu_{ei}$ is the frequency of electron–ion collisions:

$$\nu_{ei} \simeq 3 \cdot 10^{-6} \frac{n_i Z^2 \Lambda_{ei}}{T^{3/2}} \qquad \text{s}^{-1}.$$

Here $\Lambda_{ei}$ is the Coulomb logarithm for electron–ion collisions.

The term $Q_{ri}$ describes the internal energy change due to ionization and recombination processes:

$$Q_{ri} = n_e n_i \sum_z (\mathcal{K}_z^i(\tfrac{3}{2}T_e + I_z) - \mathcal{R}_z^t(\tfrac{3}{2}T_e + E^*)),$$

where $\mathcal{K}_z^i$ is the electron impact ionization rate [equation (2)], $\mathcal{R}_z^t$ is the three-body recombination through high exited levels [equation (8)], and $E^*$ is described by equation (11). The term $q_e$ in equation (23) is an electron heat conduction flux:

$$q_e = \min\begin{cases} \kappa \nabla_x T_e \\ f\sqrt{2/\pi} n_e T_e \sqrt{T_e/m_e}, \end{cases}$$

where $\kappa$ is the Spitzer's electron thermal conductivity coefficient:

$$\kappa \simeq 10^{22} \frac{T_e^{5/2}}{(Z+4)\Lambda_{ei}} \qquad \mathrm{cm^{-1}c^{-1}}.$$

The laser energy absorption is described by the term $Q_{las}$:

$$Q_{las} = k(x) I_l \left( \exp\left( -\int_{-\infty}^{x} k(x)dx \right) + \exp\left( -\int_{-\infty}^{x_{cr}} k(x)dx - \int_{x_{cr}}^{x} k(x)dx \right) \right),$$

where $I_l$ is the incident laser radiation flux and $k(x)$ is the inverse Bremsstrahlung absorption coefficient:

$$k(x) = \frac{4\sqrt{2\pi} Z^2 e^4 n_i \Lambda_{ei}}{3cT_e^{3/2} m_e^{1/2}} \frac{\left(\frac{n_e(x)}{n_{cr}}\right)^2}{\left(1 - \frac{n_e(x)}{n_{cr}}\right)^{1/2}} \qquad \mathrm{cm^{-1}}.$$

Here $c$ is the vacuum speed of light; and $n_{cr}$, $x_{cr}$ are critical density and position of the critical surface.

Special attention was paid to test this quasi-2D numerical code. It was done in three steps (Roudskoy 1992). First, the simulation of laser–plasma interaction was tested by comparing experimental results of plasma temperature measurements with calculated data in a wide region of laser parameters. Flux densities were changed from $10^{10}$ to $10^{14}$ W/cm$^2$ for Nd and Ruby glass lasers and from $10^9$ to $10^{12}$ W/cm$^2$ for $CO_2$ lasers, and pulse durations were in the interval 1 ns–1 $\mu$s. Then the simulation of an expansion stage was tested by comparing experimental and numerical time-of-flight (TOF) spectra at a distance of 1.5–3 m from a target using as initial conditions the experimental results of plasma expansion diagnostics (Zakharenkov *et al.* 1981; Golubev *et al.* 1983) corresponding to the end of a laser pulse. Finally, the results of thorough computations were compared with numerous experimental data (Sil'nov 1973; Suslov 1973; Golubev *et al.* 1988) in the region of laser pulse parameters mentioned above. The calculated data of ion charge states, ion energies, and ion currents were in a good agreement with the experimental ones that confirmed the proposed physical model. The typical results of calculations of ion spectra and average charge state distribution in plasmas are shown in figure 2.

## 5. Calculation results

A series of computations was made by varying laser pulse parameters to verify previous analytical consideration and to obtain other general dependences of highly charged ion generation in laser-produced plasmas.

First, the scaling low [equation (1)] was confirmed in the whole region of plasma parameters for both radiation wavelengths. Plasma temperatures were found to be really a function of $P_l/d$ and to increase with the increase in focal spot size if an energy flux density $I_l$ remained constant (figure 3).

The numerical calculation also supported the three-body recombination rate in an expanding plasma to follow the scaling lows [equations (18) and (19)] (figure 4). The typical value of $r_m$ is equal to a few centimeters for $\lambda = 1.06$ $\mu$m and can reach a few meters for $\lambda =$

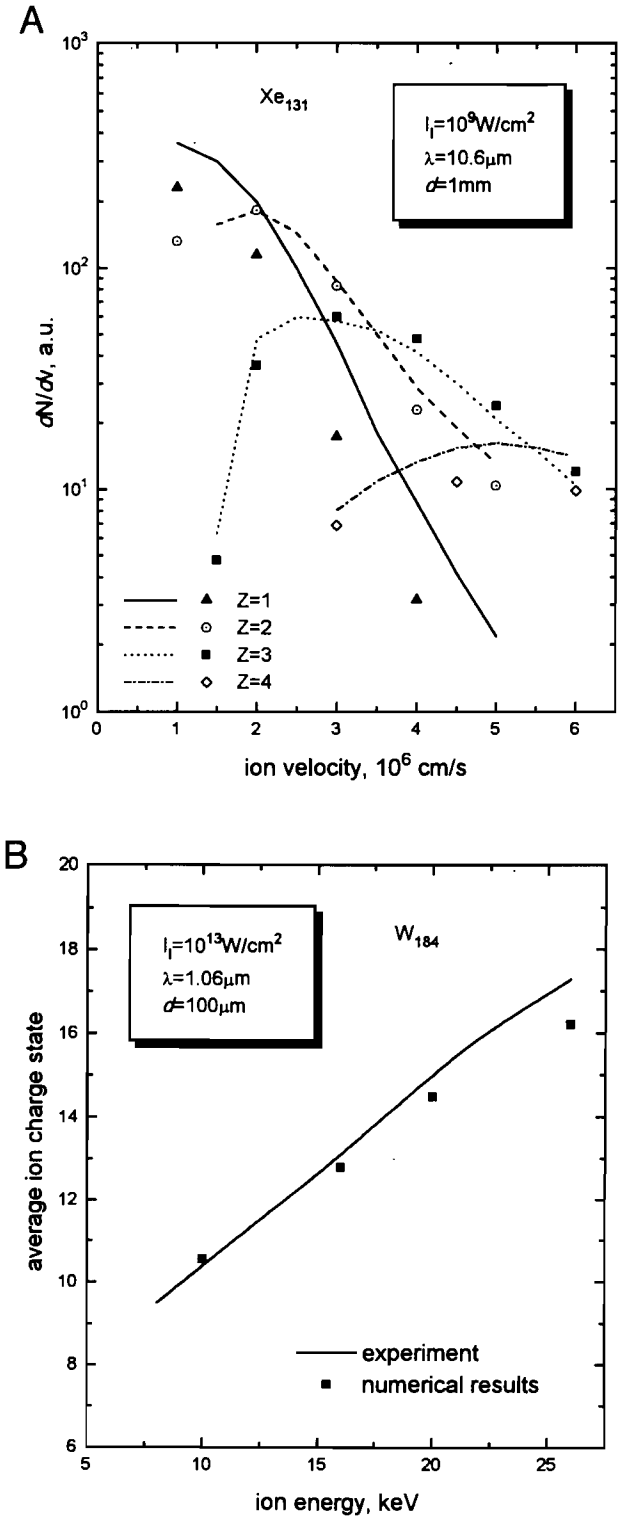


FIGURE 2. (a) Numerical (lines) and experimental (symbols) xenon ion spectra at a distance of 320 cm from the target. (b) Average charge states of wolframium ions at a distance of 350 cm from the target.

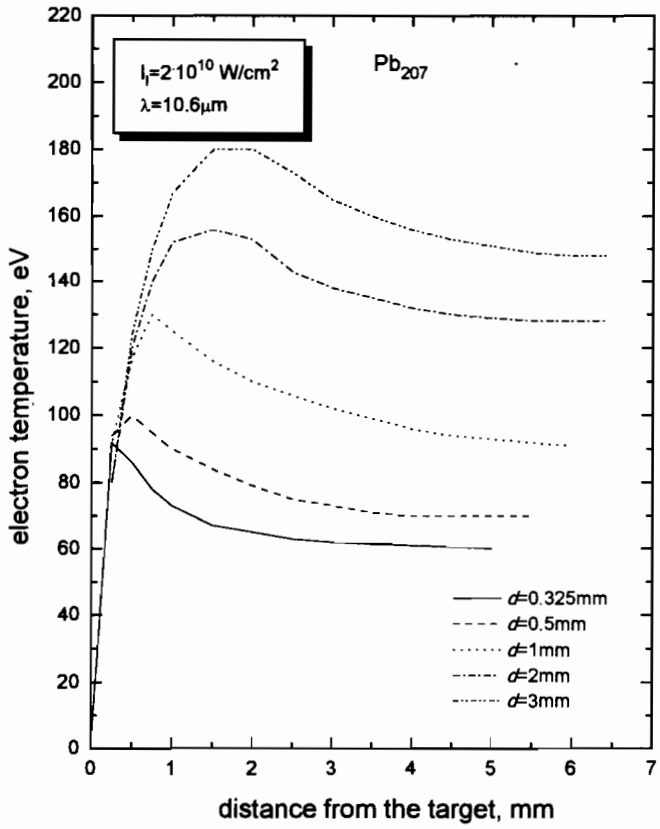


FIGURE 3. The electron temperature distribution in plasma at the moment $t = 50$ ns after beginning of laser irradiation.

10.6 $\mu$m. Ions from inner layers of the plasma cloud, possessing a smaller velocity, recombine at a greater degree than those from a periphery where ion velocities are greater. The increase in spot size and the shortening of a laser pulse lead to the increase in charge state losses. The average ion charge state evolution during plasma expansion is presented in figure 5. One can see that, in most cases, taking advantage of the higher charge states of ions in plasmas produced by Nd glass lasers is a very difficult problem; therefore, a $CO_2$ laser can be considered more preferable for higher charged ion production.

In addition, the calculation results explain the angular distribution of highly charged ions observed in experiments—the higher charged ions have the more narrow divergence angle. Really, the simulations carried out showed the ions with a higher velocity to possess a higher ratio of the normal velocity to the radial one, $u_x/u_r$. It is connected to the peculiarity of hydrodynamic acceleration of plasma ions near a flat surface. The typical value of the ratio is equal to ~1.5–2.5.

The numerical simulations revealed one more interesting relationship in the process of ion production. Ion currents proved to be largely a function of laser energy and not to depend on the focal spot size. They remain constant when the laser energy is constant and increase with the increase of the energy. Under laser power below 1 GW and spot sizes of 100 $\mu$m and above, the ion currents are directly proportional to the laser energy. But the

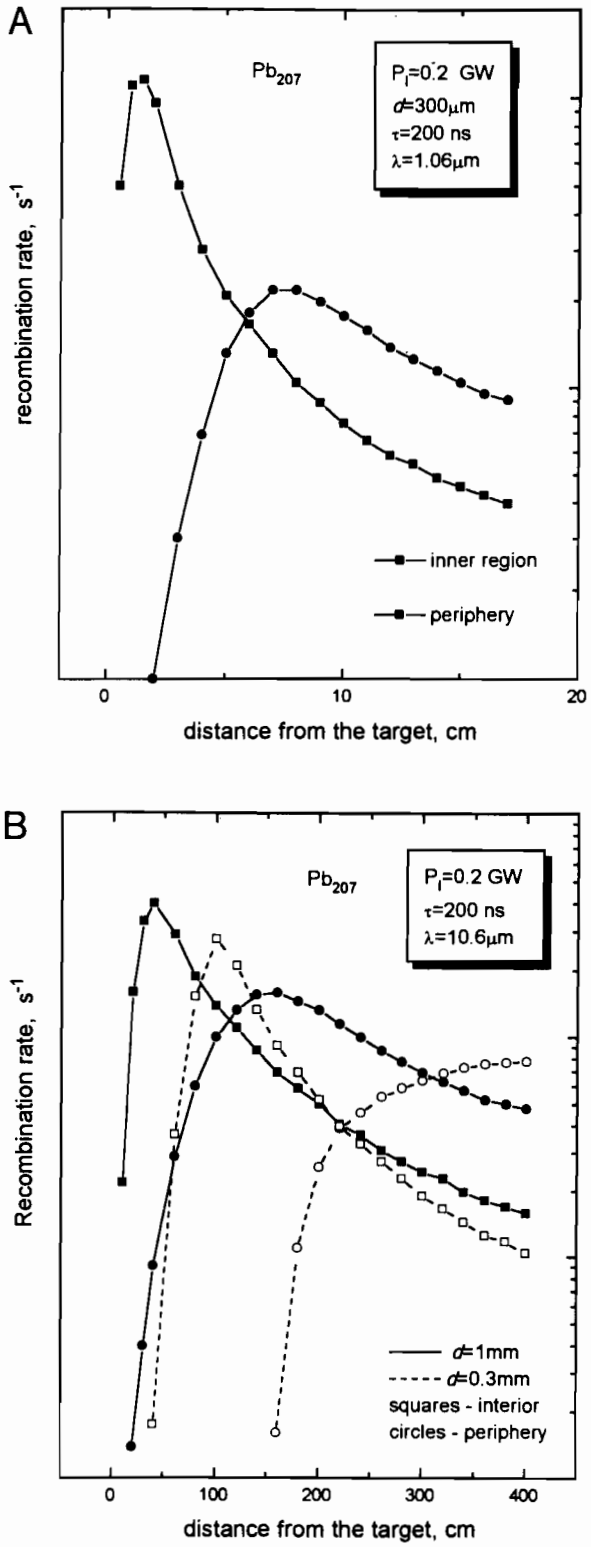


FIGURE 4. The dependence of the three-body recombination rate on the distance from the target.

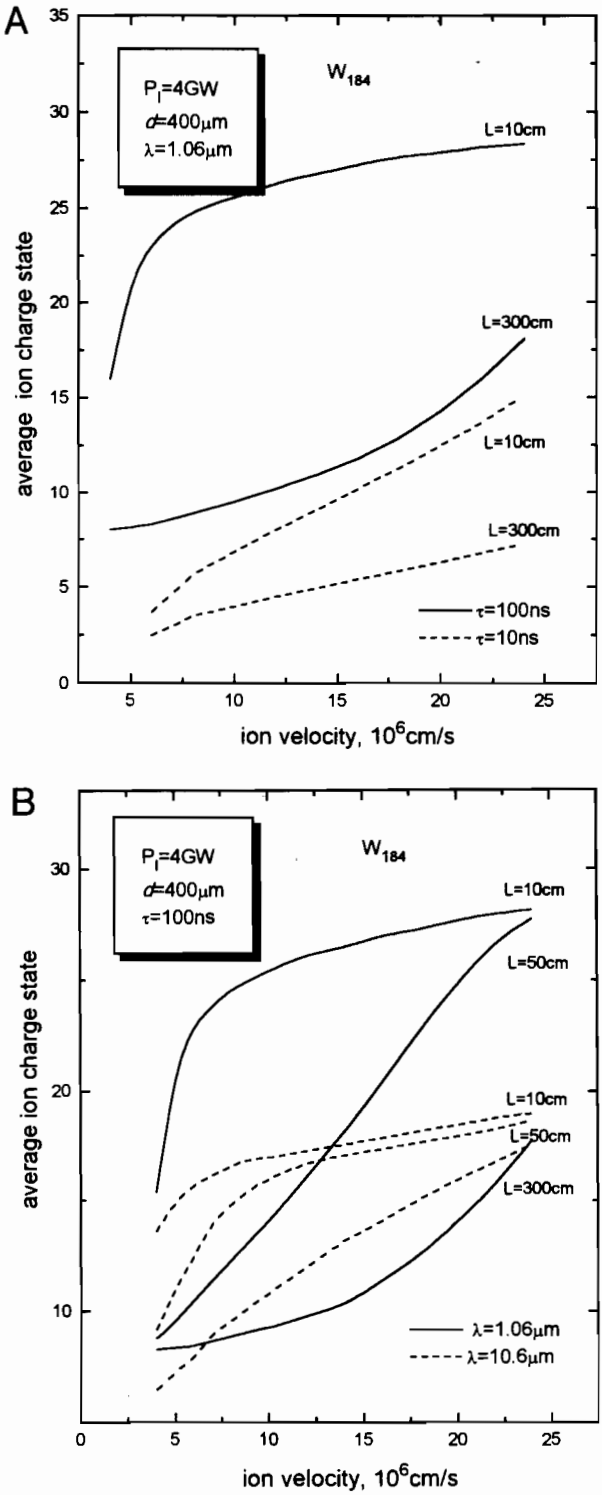


FIGURE 5. (a) The dependence of ion charge state distribution on laser pulse duration at different distances from the target. (b) The dependence of ion charge state distribution on radiation wavelength at different distances from the target.

ion current growth is retarded with the sharpening of the spot size below 50 $\mu$m. It can be conditioned by the nonlinear dependence of absorbed energy on the incident one.

Special attention was given to the influence of thermal flux restriction on a laser–target interaction. It was found that the restriction of thermal flux calls forth a steepening of the plasma density profile and the corresponding reduction of absorbed energy. Varying the factor $f$ in the range of 1–0.1 had very little effect upon plasma temperature and ion charge state distribution. The only effect consists in the reduction of the total number of ions. But the further decrease in $f$ below 0.1 leads to falling plasma temperature and ion charge states.

Finally, an attempt was made to apply the proposed model for higher flux densities. The results of calculations for $I_l \simeq 3 \cdot 10^{13}$ W/cm$^2$ and experimental data by Kozochkin *et al.* (1993) are presented in figure 6. In addition to the collisional absorption, an additional mechanism increasing a fraction of absorbed energy was assumed here as a parameter.

## 6. Conclusion

To sum up the results, the following main features of laser–target interaction were found when moderate flux intensities of incident radiation were used:

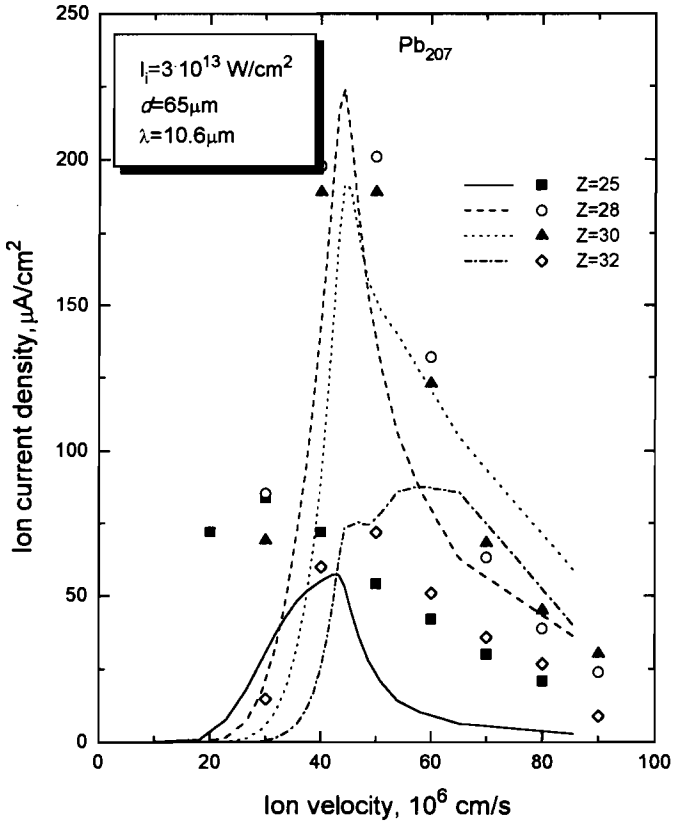


FIGURE 6. Numerical (lines) and experimental (symbols) lead ion spectra at the distance of 300 cm from the target.

- Plasma temperature on a heating stage does not depend on laser wavelengths.
- At the end of plasma heating, the charge states of ions in plasmas produced by short wavelength radiations are higher compared to those of a long wavelength radiation if the same value of $P_l/d$ is used.
- During plasma expansion into vacuum, the initial ion charge states are "frozen" at all of the initial conditions but can degrade considerably in a drift space due to three-body recombination through high exited levels.
- The rate of the recombination is higher and a position of intensive recombination is at a shorter distance from a target when a short wave radiation is used.
- An increase in a laser pulse duration increases ion energies, retards the recombination rate, and moves the intensive recombination region away from the target.
- The recombination loss drops and moves away from a target with an increase in initial plasma temperature and a decrease in focal spot size.
- The total number of ions extracted from a laser-produced plasma depends only on the absorbed laser energy.

The proposed physical model of ion generation in plasmas heated by laser radiation does not claim to be a complete description of processes in laser-produced plasma. Nevertheless, it gives a good instrument for the calculation of various plasma parameters both near a target and at a large distance from it. In addition, the disagreement of numerical and experimental data speaks for the strong effects of processes that have not been taken into account and still may be unknown, which should only inspire new investigations.

## Acknowledgment

The author would like to thank Prof. B.Yu. Sharkov and Dr. T.R. Sherwood for their encouragement of this work.

## REFERENCES

AFANASIEV, JU.V. *et al.* 1976 *Z. Exp. Teor Fis.* (*JETP*) **71**, 594.

AFROSIMOV, V.V. *et al.* 1984 *Pis'ma Z. Techn. Fiz.* (*JTP Lett.*) **10**, 1017.

ANUCHIN, M.G. *et al.* 1989 *Kv. Elektronika* (*Quant. Electron.*) **16**, 311.

BARABASH, L.Z. *et al.* 1984 *Laser Part. Beam* **2**, 49.

BARABASH, L.Z. *et al.* 1989 *Atomnaja Energija* (*Atomic Energy*) **66**, 107.

BASOV, N.G. *et al.* 1983 *Z. Exp. Teor Fis.* (*JETP*) **84**, 564.

BASOV, N.G. *et al.* 1986 *Heating and Compression of Thermonuclear Targets by Laser Beams.* (Cambridge University Press, New York).

DEMCHENKO, N.N. 1988 *Kv. Elektronika* (*Quant. Electron.*) **15**, 1305.

GOFORTH, R.R. & HAMMERLING, P. 1976 *J. Appl. Phys.* **47**, 3918.

GOLUBEV, A.A. *et al.* 1983 Preprint ITEP-175 (Moscow).

GOLUBEV A.A. 1984 *Kv. Elektronika* (*Quant. Electron.*) **11**, 1854.

GOLUBEV, A.A. *et al.* 1988 Preprint ITEP-134 (Moscow).

GUREVICH, A.V. & PITAEVSKY, L.A. 1964 *Z. Exp. Teor. Fiz.* (*JETP*) **46**, 1281.

GUS'KOV, S.YU. *et al.* 1983 *Kv. Elektronika* (*Quant. Electron.*) **10**, 802.

HORA, H. *et al.* 1992 *Chech. J. Phys.* **42**, 927.

KOZOCHKIN, S.M. *et al.* 1993 Preprint IAE-5635/7 (Moscow).

LATYSHEV, S.V. & ROUDSKOY, I.V. 1985 *Fiz. Plasmy* (*Plasma Phys.*) **11**, 1175.

LATYSHEV, S.V. & ROUDSKOY, I.V. 1986 Preprint ITEP-2 (Moscow).

LATYSHEV, S.V. & ROUDSKOY, I.V. 1987 Preprint ITEP-120 (Moscow).

McWirter, R. 1965 *Plasma Diagnostic Techniques*, R.H. Huddlestone and S.L. Leonard, eds. (Academic Press, New York), p. 21.

Payne, G.L. *et al.* 1978 *J. Appl. Phys.* **49**, 4688

Roudskoy, I.V. 1992 Doctor Thesis, Phys. Soc., Moscow.

Sil'nov, S.M. 1973 Doctor Thesis, MIPI, Moscow.

Suslov, A.I. 1973 Doctor Thesis, MIPI, Moscow.

Tallents, G.J. 1980 *Plasma Phys.* **22**, 709.

Veinstein, L.A. *et al.* 1979 *Exitation of Atoms and Broadening of Spectrum Lines.* (Nauka, Moscow).

Volenko, V.V. *et al.* 1983 *Kv. Elektronika* (*Quant. Electron.*) **10**, 1281.

Zakharenkov, Yu.A. *et al.* 1981 Preprint FIAN-126 (Moscow).

Zeldovich, Ya.B. & Raizer, Yu.P. 1966 *Physics of Shock Waves and High Temperature Hydrodynamic Phenomena.* (Nauka, Moscow).